J. Comput. Appl. Res. Mech. Eng. Vol. 11. No. 1, pp. 127-138, 2021 *DOI: 10.22061/JCARME.2020.6737.1860*

Journal of Computational and Applied Research in Mechanical Engineering

jcarme.sru.ac.ir

SRTTU

JCARME

ISSN: 2228-7922

Research paper

Numerical investigation and optimization of the mechanical behavior of thin-walled tubes with combined geometric

F. Kholoosi, S. Jafari and M. Karimi*

Mechanical Engineering Department, Bu-Ali Sina University, Hamedan, 65175-38659, Iran

Article info:

Article history:

Received: 06/04/2020

Revised: 22/06/2020

Accepted: 25/06/2020

Online: 28/06/2020

Keywords:

Mean crushing force,
Combined geometric,
Optimization,
NSGA-II algorithm,
Thin-walled.

***Corresponding author:**
karimi_mh@yahoo.com

Abstract

In this study, the crushing behavior and energy absorption of various thin-walled structures under quasi-static loading are investigated. Some experimental data from similar work are used for the validation of a simulated model. Some samples are designed and considered with different combined geometries. It was found from simulated model that the most ability of specific energy absorption and crushing force efficiency are related to the circle-square sample. For the circle-square sample, the analytic equations for calculating the mean crushing force are obtained. The mean crushing force result is compared with the result of simulations, showing a good agreement. The multi-objective optimization process for the circle-square structure is performed using non-dominated sorting genetic algorithms for two statuses. The purpose of optimization is to increase the specific energy absorption and to decrease the peak crushing force, which causes the increase of the crushing force efficiency amount. The amount of specific energy absorption in the second status compared to the first status is improved by 17%. The amount of crushing force efficiency is improved by 12% after the optimization process.

1. Introduction

Energy absorbers are very important due to having many applications in different industries such as automobile, aircraft, etc. One of the uttermost usages of the absorbers is related to the thin-walled structures. So far, much research has been done on thin-walled structures. Alavi Nia and Hamedani [1] investigated the deformation of shape and capacity of energy absorptions of thin-walled structures with different cross-sections (circle, rectangular, hexagonal, triangle, pyramidal, and cone) using numerically as well as experimentally approaches. The tested structures had the same material and were loaded by quasi-static axial loading. They knew that the geometry of the cross-section has a significant effect on energy absorption and circle cross-section have the most capacity on energy absorption among different cross-sections. Zhang and Yu [2] investigated the energy absorption of a circle thin-wall tube in 2009. Niknejad et al. [3] considered the theory of multi-cells hexagonal MCF in the corrugated

tubes filled with polyurethane foam. Zhang et al. [4-6] investigated the axial crush with multi-cells. Tabacu [7] analyzed the circle tubes with the rectangular cell. In 2019, Xu et al. [8] considered the crushing behavior of multi-cell structures. Chen et al. [9] considered the behavior of thin-walled structures with multi-cell sections. After that, they compared theoretical and simulation results. Guan et al. [10] studied the absorbed energy of circular tubes with splitting multiple under the impact loading. After that, they compared the result of their theoretical, experimental, and simulation studies. In another study, Zhang et al. [11] investigated the energy absorption of different circular structures. Tran [12] studied the crush of multi cell structures with some holes on their walls. Li et al. [13] considered the crushing of reinforced multi-cell structures. In this study, they proposed an analytical equation and compared its result with theoretical and simulation results. Some researchers optimized the sample structure geometries using the multi-objective particle swarm optimization (MOPSO) [14, 15] as well as the non-dominated sorting genetic algorithm (NSGAII) [16]. Tran et al. [17, 18] considered the crushing behavior and numerical optimization of multi-cell structures. Qiu et al. [19] proposed an analytical equation for calculating the mean crushing force (MCF) of multi-cells hexagonal absorptions using the MOPSO method. They optimized the structure geometries. Xu et al. [20, 21] submitted a design for the energy absorption in the metro and considered the possibility of its optimization using the multi objective genetic algorithm (MOGA). In another study, the structures with functional grade structures (FGS) material were investigated and later one FGS structure was optimized using NSGA-II algorithm [22]. In one study, Shen and et al. [23] considered the crush behavior of structure with multi-cell rectangular cross section, and the proposed structure was optimized using the NSGA-II. In another study, Zhang et al [24] considered the thin-walled tubes with the multi-cell rectangular cross-section and compared the results of their simulations with the experimental results. Some researchers are focusing on optimization of different thin-walled structures [25, 26]. Chen et al. [27] optimized their structure using the MOPSO. Abolfathi and Alavi Nia [28, 29] proposed a new design for thin-walled structures using the MOPSO method. It was found that the optimization process can increase the amount of specific energy absorption (SEA), and it also can decrease the peak crushing force (PCF). Acar et al. [30] introduced their multiple structures with circular sections. They investigated two important performances of the energy absorption (crushing force efficiency (CFE & SEA) for their structures. Finally, they optimized their structures. Pirmohammad and Marzdashti [31] simulated their structures before and after optimized structures using the NSGA-II algorithm.

In the present study, various models with combined geometries are proposed, and for validation purposes, experimental data from Ref. [6] are used. Then, using the proposed formula proposed by Zhang et al. [4, 6], the analytic formula for the circle-square model is submitted. After that, the effect of geometric parameters on the amount of MCF and SEA are investigated. The thin-walled structure's absorbing energy aims to increase the SEA and to decrease the PCF so that the CFE can be increased. Therefore, to increase the SEA and decrease the PCF, which cause an improvement of the CFE, the optimization process using the NSGA-II algorithm is employed.

2. Simulation

2.1. Validation

Using the finite element software, Ls-Dyna, double and quadruple cell profiles proposed by Zhang and Zhang [6] were investigated numerically in the present study. The used material was aluminum AA6061-O with the E= 68 GPa, σ_y= 71 MPa, σ_u= 159.9 MPa, ρ=2700 kg/m^3, and υ = 0.33 [6]. In the Ls-Dyna software, the piecewise linear plasticity option was selected. The diameter, length, and thickness of the cylinder were 36, 120, and 1.2 mm, respectively. The characteristic size of the mesh was 1.5 mm for all samples. The perimeters of all experimental samples from Ref. [6] were welded to the lower surface. In the simulation of the present study, 6 mm of the lower surface was constrained in all directions. The contact automatic single surface option from the

software was used for describing the contact between the elements of the thin-walled surface as well as for describing the contact between the striker and the thin-walled structure. The speed was the same as what reported in Ref. [6]. Fig. 1 shows the double and quadruple cell profiles given in Ref. [6] and the present study.

Fig. 2 shows the final stage of the cross-section of the profiles under the quasi-static loading. In both samples, after the beginning of loading, the fold began from the place of impact and continued up to final deformation of the sample. According to Fig. 2, in both experimental methods [6] and present simulation, the amount of deformation in quadruple cell profile is less than double cell profile. The results of the present simulation and experimental methods [6] are shown in Fig. 3 and compared in Table 1. The parameters of MCF, PCF, and SEA are calculated for comparison of both profiles' performances.

(a) (b)

Fig. 1. Double and quadruple cell structure; (a) present simulation and (b) experimental samples [6].

Fig. 2. Deformation mode of double and quadruple experimental cell structure [6] and present simulation.

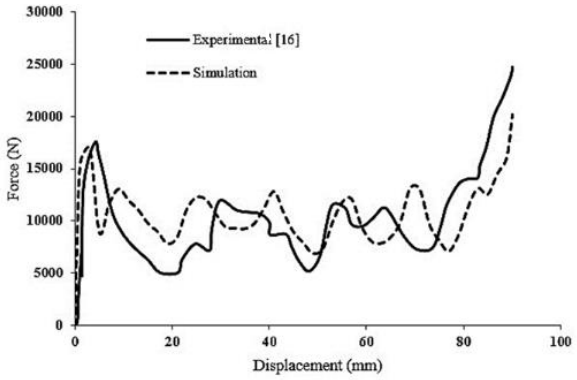

(a)

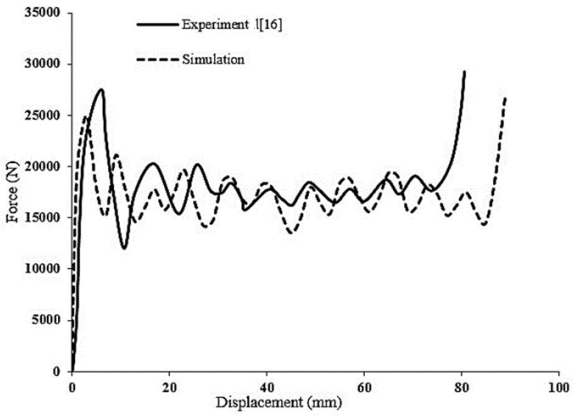

(b)

Fig. 3. Force-displacement curves of experimental [6] and present simulation; (a) double cell and (b) quadruple cell.

2.2. Considering some other models with combined geometric

Some other various models such as Circle-Square (CS), Circle-Rectangular (CR), Circle-Triangular (CT), Circle-H-Shape (CHS), and Circle-Hexagonal (CH) were considered for simulation. Fig. 4 shows all models with the same height, diameter, thickness, and even loading condition. In all models, D=36 mm, L=120 mm, and t=1.2 mm.

Table 1. Experimental [6] and numerical results.

Specimen	Experimental result [6]			Numerical result			Error (%)		
	PCF (kN)	MCF (kN)	SEA (J/gr)	PCF (kN)	MCF (kN)	SEA (J/gr)	PCF	MCF	**SEA**
Double cell	17.50	10.70	21.02	16.90	10.57	21.80	3.40	1.20	4.10
Quadruple cell	27.20	18.02	30.02	25.01	18.87	31.47	8.02	4.70	4.80

The structures were made from Al-3003-H12; the material properties are given in Table 2 [1]. Fig. 5 shows the amount of final deformation length by quasi-static loading. It can be observed that the maximum deformation length corresponds to the CS model, while the minimum one corresponds to the CR model.

In Fig. 6, the force-displacement diagram resulted from the simulation is shown for each model. For all models, the force is increased linearly up to peak value, and once the first folding is observed, the amount of force is decreased. Totally, the kinetic energy of the striker is converted to plastic deformation like folding.

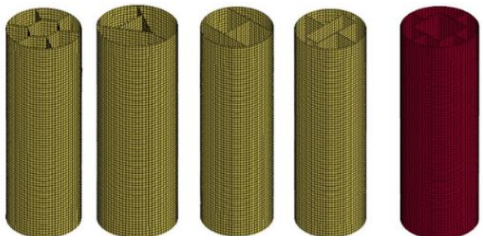

(a) (b) (c) (d) (e)

Fig. 4. Simulated models; (a) CH, (b) CT, (c) CHS, (d) CR, and (e) CS.

Table 2. Al-3003-H12 properties [1].

$\rho\left(\frac{Kg}{m^3}\right)$	E(GPa)	υ	σ_y(MPa)	$\sigma_{ultimate(MPa)}$	$\varepsilon_{ultimate}$
2700	68	0.3	130	137.5	**0.24**

(a) (b) (c) (d) (e)

Fig. 5. Deformation mode: (a) CT; (b) CHS; (c) CR; (d) CH, (e) CS.

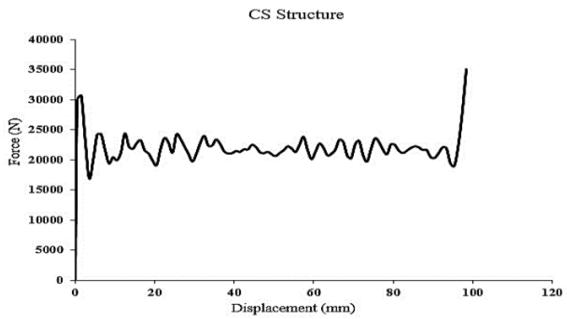

(a)

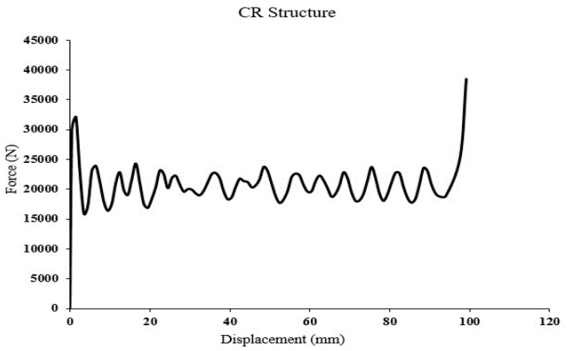

(b)

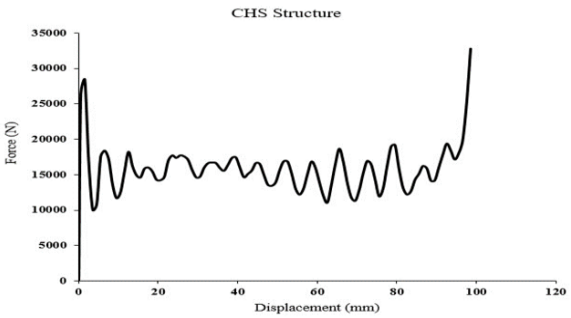

(c)

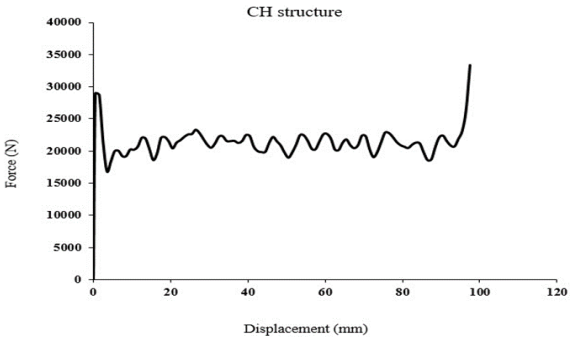

(d)

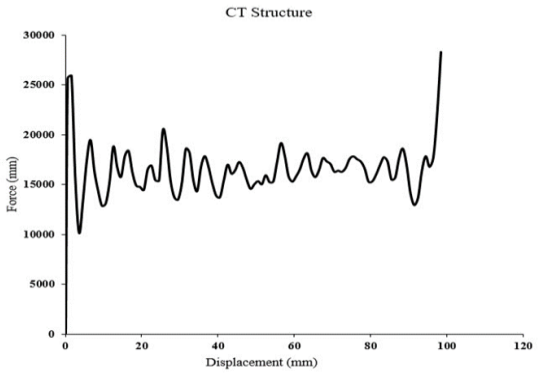

(e)

Fig. 6. Force-displacement diagrams of simulation: (a) CS; (b) CR; (c) CHS; (d) CH, and (e) CT.

According to Fig. 6, it is clear that the maximum loading amount of crush is corresponding to the CS model, while the minimum loading amount is corresponding to the CT model.
Table 3 shows the results of all model simulations. In the present study, some of the main parameters such as SEA, PCF, CFE, MCF, deformed mass, and energy absorption (EA) are considered.
SEA was used as one of the main parameters for measuring the amount of energy absorbed in the used structure. It is calculated by Eq. (1)

$$SEA = \frac{U}{m} = \frac{P_m . \delta_c}{m} \quad (1)$$

In this formula, m is the mass of the crushed structure and δ_c is the crush (deformation) length. It was seen that the maximum of SEA corresponds to CS and CH models, while the minimum corresponds to CHS and CT models. By decreasing the deformation mass and increasing the MCF, the amount of SEA in the models is increased. The other main factor used in evaluating the energy absorption performance is the CFE. It is calculated according to Eq. (2):

$$CFE = \frac{F_{mean}}{F_{max}} \times 100 \quad (2)$$

By increasing CFE, the model is desirable for better energy absorption. The CS model has the most amount of CFE, while the CHS has the lowest amount. The lowest amount of MCF corresponds to CHS, while the most amount corresponds to CS one. The maximum amount of PCF corresponds to CR model, while the minimum amount corresponds to CT one. Therefore, the CS model is the best energy absorber.

3. Theoretical analysis

3.1. CS model

The MCF is calculated by Eq. (3) (using the balance energy):

$$k. P_m. 2H = E_b + E_m \quad (3)$$

In this equation, k is the effective crushing distance coefficient, 2H is the wavelength, E_b is the bending energy, and E_m is the membrane deformation energy. For calculating the mean energy two methods were used.

3.1.1. The First Method

In this method, by using an equation proposed by Zhang et al. [4], the MCF is calculated. The bending energy is calculated by Eq. (4):

$$E_b = 2\pi M_o L_c \quad (4)$$

In this equation, the amount of $L_c = \pi D + 4(b_1+b_2)$ is equal to the whole length of the cross-section, according to Fig. 7.

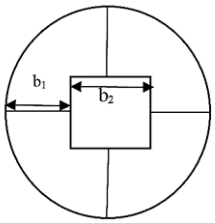

Fig. 7. Cross section of the CH structure.

The amount of Mo is calculated by Eq. (5):

$$M_0 = \frac{\sigma_0 t^2}{4} \quad (5)$$

Table 3. The results of simulation of energy absorber profiles with different geometries.

	specimen	EA (J)	PCF (kN)	MCF (kN)	δ_c (mm)	Mass (gr)	Deformed mass (gr)	CFE (%)	SEA (J/g)
1	CS	2370	30.7	23.9	103	85.9	73	77	32.465
2	CR	1930	32.7	20.52	92.5	85.9	66	62	29.242
3	CHS	1640	28.4	16.27	100.5	75.2	63	57	26.031
4	CH	2100	28.9	21.18	97.5	86.7	70	73	29.975
5	CT	1670	25.9	16.60	99.5	73.3	60	64	27.833

The flow stress is calculated by Eq. (6) [32]:

$$\sigma_0 = \frac{\sigma_u + \sigma_y}{2} \quad (6)$$

The membrane deformation energy is calculated by the following three steps. First, the tube's membrane energy during a complete folding formation is calculated by Eq. (7) [7]:

$$E_{m,tube} = 2\pi N_o H^2 = 8\pi M_o H^2 / t \quad (7)$$

In this equation, $N_o = \sigma_o t$ is the fully plastic force per unit length. In the second step, for calculating the membrane deformation energy of T- shape element, Eq. (8) is used [4]:

$$E_{m,T\text{-}shape} = 2N_o H^2 = 8M_o H^2/t \quad (8)$$

In the third step, Eq. (9) is used for calculating the membrane deformation energy of the corner element.

$$E_{m,corner} = 4M_o H^2/t \quad (9)$$

Using the proposed three equations and substituting in Eq. (3), Eq. (10) is obtained. After simplifying Eq. (10), the MCF is calculated by Eq. (11):

$$k.P_m.2H = 2\pi M_o [\pi D + 4(b_1+b_2)] + 105.13 M_o H^2/t \quad (10)$$

$$P_m = EC \times \frac{6.42}{k} \sigma_o t^{1.5} [\pi D + 4(b_1 + b_2)]^{0.5} \quad (11)$$

In Eq. (11), EC is the enhancement coefficient. For specifying the effect of inertia and the strain rate, Langseth and Lademo [33], Langseth and Hopperstad [34], and Zhang et al. [4] suggested that the revised coefficient can be selected as $1.3<EC<1.6$.

3.1.2. Second method

In 2014, Zhang & Zhang [6] proposed another method for calculating the membrane deformation energy for T-shape element, as follows in Eq. (12):

$$M_{T-Shape} = \frac{64.9\, M_o H^2}{t} \cdot \frac{1}{\left(\frac{B}{t}\right)^{0.6}} \quad (12)$$

For calculating the membrane deformation energy of 180° corner element, Eq. (13) was proposed from [6]:

$$M_{corner(180^\circ)} = \frac{24.4\, M_o H^2}{t} \cdot \frac{1}{\left(\frac{B}{t}\right)^{0.6}} \quad (13)$$

The B amounts are shown in Fig. 8 from [6]. Then by replacing the element amounts in Eq. (3), it reaches Eq. (14):

$$k.P_m.2H = 2\pi M_o [\pi D + 4(b_1+b_2)] + 60.5\, \sigma_o H^2 t \quad (14)$$

By simplifying Eq. (14), the MCF is calculated by Eq. (15).

$$P_m = \frac{9.7}{k} \sigma_o t^{1.5} [\pi D + 4(b_1 + b_2)]^{0.5} \quad (15)$$

3.2. Comparing the analysis and simulation results

In this part, the results of the analytic formulation are compared with the simulation result. As shown in Table 4, the result of analytic formulation conform the simulation result.

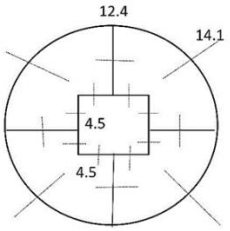

Fig. 8. Division of constituent elements and parameter B of each element in CS structure.

Table 4. Comparison between theoretical and numerical results.

	MCF	Value (kN)	Error (%)
1	$MCF_{, theory1}$	19.53	-22.3
2	$MCF_{, theory1}$ EC=1.3)	25.3	5.5
3	$MCF_{, theory1}$ EC=1.4)	27.3	12.4
4	$MCF_{, theory2}$	29.5	18.9

The simulation amount of MCF is 23.9kN. In the first theory (Eq. (11)), the MCF is calculated as 25.3kN using EC of 1.3, resulting in a 5.5% error between the formula and simulation results.

4. Optimization

In this part, the CS structure is optimized by the NSGA-II. In Eq. (7), the EC of 1.3 is used for optimizing. Two objective functions were considered for this purpose. The first objective function is defined as the PCF. The PCF in collapsing energy absorbers is related to the deformation of the elastic area that is decreased quickly after beginning the plastic deformation. The second objective function is defined as the SEA calculated by SEA=U/m. This kind of algorithm minimizes the amount of objective functions [35]. Therefore, by inversing the second objective function, the minimum amount shall be its maximum. The designing variables and the upper and lower bounds of them are listed in Table 5.

The design variables domain should be selected in a way that its ratio will be, and so that the structure will be considered thin-walled. For the optimization process, the equality constraint is considered according to Eq. (16). However, the mass of the thin-walled structure is low, the amount of mass as inequality constraint is considered less than 0.09 kg in the design process. In the equality constraint, the length of the two sides, b_1 and b_2 should be equal to its diameter as Eq. (16).

$$b_1+b_2=D \tag{16}$$

NSGA-II algorithm is one of the simplest and most applicable multi-objective optimizing algorithm that nowadays is used by different researchers. In this part, optimization is used in two ways using NSGA-II.

In the first status, optimization is performed by using the NSGA-II algorithm. In the other status, the optimization of NSGA-II is performed better by using the fgoalattain command in MATLAB. The optimization setting is performed based on Table 6. Fig. 9(a and b) show the pareto diagrams for the first and second optimization, respectively. The selection criteria for selecting the optimized point is considered in a way that PCF have the lowest amount while, SEA has the maximum possible amount and CFE will be near to 1.

It can be observed from Fig. 9. that by selecting one point in Fig. 9(a) and one point in Fig. 9(b) as the optimized point, it satisfies the mentioned conditions. Now, by using the 3D diagram in Fig. 10, the effect of geometric parameters in PCF and SEA is considered. At first, the geometric parameters on the PCF are considered. According to Fig. 10(a), by increasing the amounts of b_1 and b_2, the amount of PCF is increased with rete 1.

Table 5. The initial designs and ranges of variables.

Design variable	Initial design	lb	ub
D (mm)	36	30	44
t (mm)	1.2	1	1.6
L (mm)	120	80	160
b_1 (mm)	9	7	11
b_2 (mm)	18	16	20

Table 6. Parameters for NSGA-II algorithm.

Parameters	Value
Population	50
Pareto	0.7
Generation	100
Constrain	1e-9
Function	1e-8

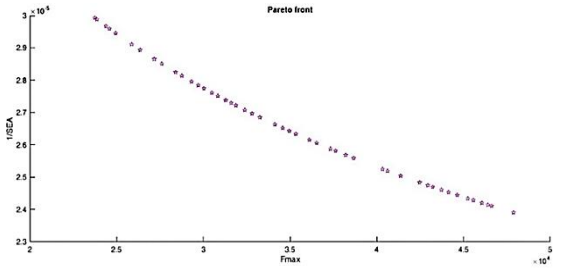

(a)

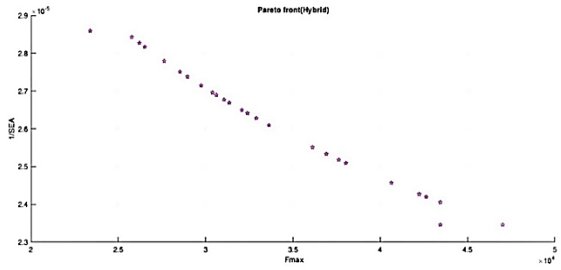

(b)

Fig. 9. Pareto frontier for optimization; (a) NSGA II and (b) hybrid.

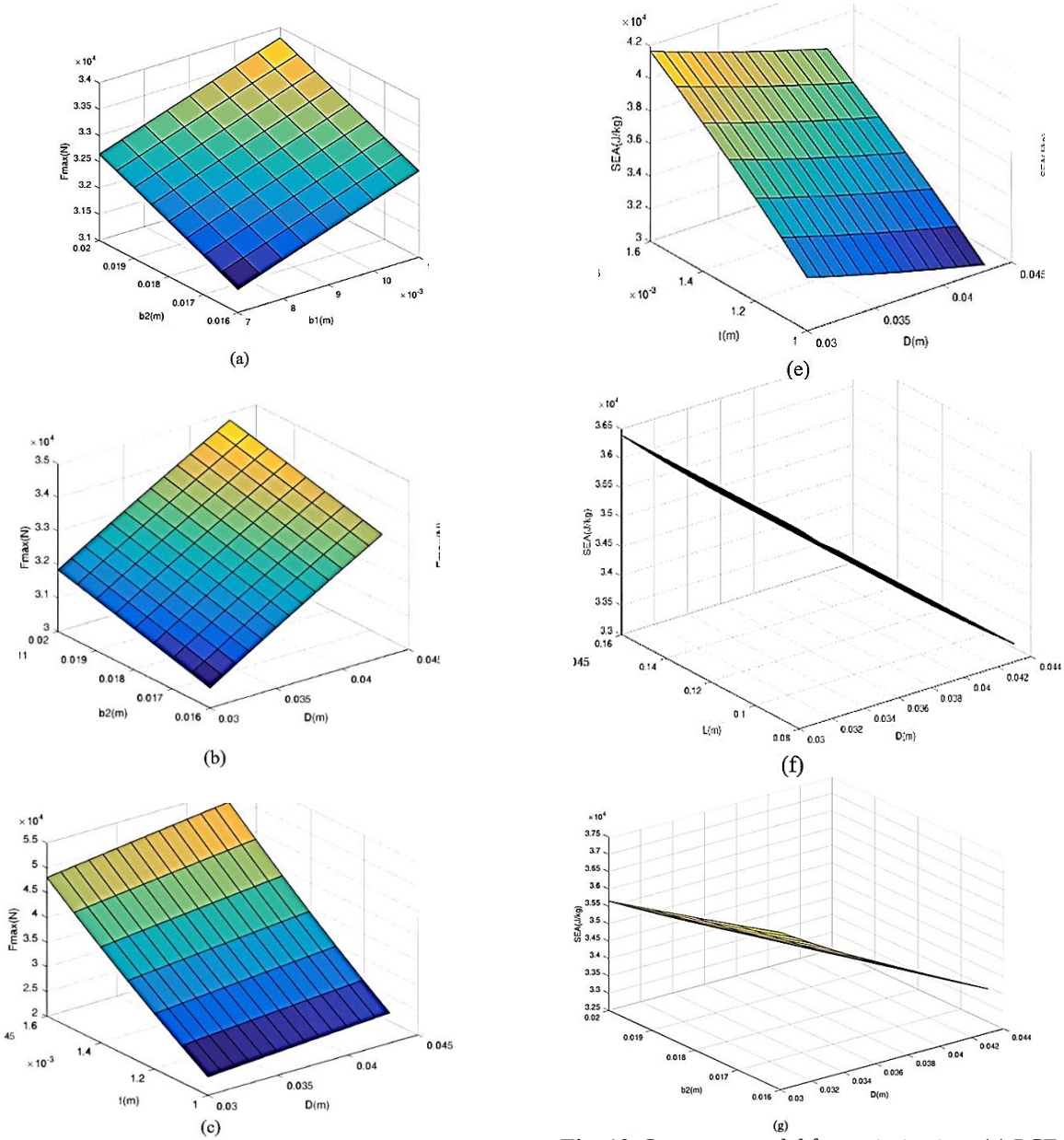

Fig. 10. Surrogate model for optimization; (a) PCF of b_1 and b_2, (b) PCF of b_2 and D, (c) PCF of t and D, (d) SEA of t and L, (e) SEA of t and D, (f) SEA of L and D, and (g) SEA of b_2 and D.

According to Fig. 10(b), by increasing the amount of parameters D and b_2, diameter and square's side, the amount of PCF is increased. It is found that by increasing these two parameters, the PCF is increased. According to Fig. 10(c), having two parameters of t and D, it is found that the effect of thickness in the optimization process is more than the effect of diameter, and it causes more increase in the crushing force. Now, the SEA is considered. According to Fig.

10(d) and by considering two parameters of L and t, it becomes more clear that the height of the structure has no effect on the SEA, and also by increasing the thickness, the amount of SEA is increased. Regarding the effects of t and D on the optimization process, it can be observed in Fig. 10(e) that by increasing the diameter of the energy absorption tube, the amount of SEA is reduced. But by increasing its thickness, the amount of SEA is increased. Fig. 10(f) shows the effect of simultaneous effect of two parameters D and L. It shows that by increasing the diameter, the amount of SEA is decreased and the height has no effect on the SEA. According to Fig. 10(g), considering two parameters of D and b_2, simultaneously, it shows that by increasing the diameter, the amount of SEA is decreased. Meanwhile, the square's side d effect on the ratio of diameter on the result. In the second status, the optimization algorithm was performed in the Matlab software using fgoalattain command and parameters in Table 6. The result of both optimized methods compared to the simulation mode are summarized in Table 7.

Now, by using the optimized values of design variables, the numerical analysis is performed again. Fig. 11 shows the diagram of force displacement resulted from the simulation of optimized values.

In Table. 8, the result of optimizing the CS model is shown. As it shows, in the first step, the SEA is increased to 8.4%, and in the second step, it is increased to 16.96%. In a comparison of the primal model, CFE in the first step is improved near to 5%, and in the second step, it is improved near to 12%.

Table 7. Optimized varibles obtained from NSGA-II and fgoalattain algorithms (Hybrid).

Variable	Initial design (mm)	NSGA-II (mm)	Hybrid (mm)
D	36	33.11	31.5
T	1.2	1.00	1.25
L	120	80.10	81.40
b_1	9	8.295	7.50
b_2	18	16.52	16.51

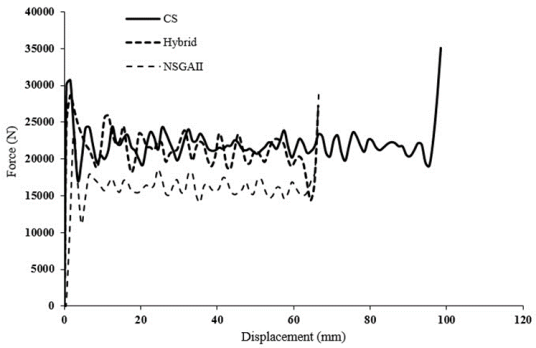

Fig. 11. Force-displacement curves of simulation and optimizations.

Table 8. Comparison between optimization results and FE values.

Variable	Initial design	NSGA-II	Hybrid
Mass(gr)	85.9	43.9	53.5
MCF	23.9	19.43	25.35
PCF	30.7	23.7	28.6
SEA(J/g)	32.465	35.475	39.130
CFE (%)	77	81.9	88.63

4. Conclusions

According to the performed validation, comparison of the simulation result and the experimental result of Zhang show suitable conformity; therefore, it can be confirmed that the simulation is done correctly. By considering the proposed models, the maximum of the SEA and CFE are related to the CS model, while the minimum amount is related to the CHS. So the best model among the offered ones is the CS model. The proposed analytic equation has suitable conformity with the result of the simulation. By considering the effective parameters on crushing force and SEA, the height does not effect on the objective function. By increasing the diameter, the PCF increases, and SEA decreases. By increasing thickness, the PCF and SEA increase. Generally, thickness is more effective than the other geometric parameters such as the diameter of the circle and the length of the square's side. In the optimization part, by using the performed optimization, the SEA in the first and second steps increase to 8.4% and 16.96%, respectively. The CFE in the first model is 81.9% instead of 77% and in the second model, it is 88.36% instead of 77%.

References

[1] A. Alavi Nia and J. H., Hamedani," Comparative analysis of energy absorption and deformations of thin walled tubes with various section geometries", *Thin-Walled Struct.*, Vol. 48, No. 12, pp. 946–954, (2010).

[2] X. W. Zhang and T. X. Yu, "Energy absorption of pressurized thin-walled circular tubes under axial crushing", *Int. J. Mech. Sci.*, Vol. 51, No. 5, pp. 335-349, (2009).

[3] A. Niknejad and M. M. Abedi and G.H. Liaghat and M. Zamani Nejad, "Prediction of the mean folding force during the axial compression in foam-filled grooved tubes by theoretical analysis", *Mater. Des.*, Vol. 37, pp. 144–151, (2012).

[4] X. Zhang and G. Cheng and H. Zhang," Theoretical prediction and numerical simulation of multi-cell square thin-walled structures", *Thin-Walled Struct.*, Vol. 44, No. 11, pp. 1185-1191, (2006).

[5] X. Zhang and H. Zhang, "Energy absorption limit of plates in thin-walled structures under compression", *Int. J. Impact Eng.*, Vol. 57, pp.81-98, (2013).

[6] X. Zhang and H. Zhang, "Axial crushing of circular multi-cell columns", *Int. J. Impact Eng.*, Vol. 65, pp. 110-125, (2014).

[7] S. Tabacu, "Axial crushing of circular structures with rectangular multi-cell insert", *Thin-Walled Struct.*, Vol. 95, pp. 297–309, (2015).

[8] X. Xu, Y. Zhang, X. Chen, Z. Liu, Y. Xu and Y. Gao, "Crushing behaviors of hierarchical sandwich-walled columns", *Int. J. . Mech. Sci.*, Vol. 161, pp. 105021, (2019).

[9] T. Chen, Y. Zhang, J. Lin and Y. Lu, "Theoretical analysis and crashworthiness optimization of hybrid multi-cell structures", *Thin-Walled Struct.*, Vol. 142, pp. 116–131, (2019).

[10] W. Guan, G. Gao, and T. Zhuo, "Theoretical, experimental and numerical investigations on the energy absorption of splitting multiple circular tubes under impact loading", *Thin–Walled Struct.*, Vol. 155, 106916, (2020).

[11] D. Zhang, G. Lu, D. Ruan and Q. Fei, "Energy Absorption in the Axial Crushing of Hierarchical Circular Tubes", *Int. J. Mech. Sci.*, Vol. 171, 105403, (2020).

[12] T. Tran, "Study on the crashworthiness of windowed multi-cell square tubes under axial and oblique impact", *Thin–Walled Struct.*, Vol. 155, pp. 106907, (2020).

[13] Z. Li, W. Ma, L. Hou, P. Xu and S. Yao, "Crashworthiness analysis of corrugations reinforced multi-cell square tubes", *Thin–Walled Struct.*, Vol. 150, pp. 106708, (2020).

[14] J. Fang, Y. Gao, G. Sun, N. Qiu and Q. Li, "On design of multi-cell tubes under axial and oblique impact loads", *Thin-Walled Struct.*, Vol. 95, pp. 115-126, (2015).

[15] F. Xu, "Enhancing material efficiency of energy absorbers through graded thickness structures", *Thin-Walled Struct.*, Vol. 97, pp. 250–265, (2015).

[16] Q. Gao, L. Wang, Y. Wang and C. Wang, "Crushing analysis and multi objective crashworthiness optimization of foam-filled ellipse tubes under oblique impact loading", *Thin-Walled Struct.*, Vol. 100, pp. 105–112, (2016).

[17] T. Tran, S. Hou, X. Han, N. Nguyen and M. Chau, "Theoretical prediction and crashworthiness optimization of multi-cell square tubes under oblique impact loading", *Int. J. Mech. Sci.*, Vol. 89, pp. 177—193, (2014).

[18] T. Tran, S. Hou, X. Han and M. Chau, "Crushing analysis and numerical optimization of angle element structures under axial impact loading", *Compos. Struct.*, Vol. 119, pp. 422–435, (2015).

[19] N. Qiu, Y. Gao, J. Fang, Z. Feng, G. Sun and Q. Li., "Theoretical prediction and optimization of multi-cell hexagonal tubes under axial crashing", *Thin-Walled Struct.*, Vol. 102, pp. 111–12, (2016).

[20] P. Xu, C. Yang, Y. Peng, S. Yao, D. Zhang and B. Li, "Crash performance and multi objective optimization of a gradual energy-absorbing structure for subway vehicles", *Int. J. Mech. Sci.*, Vol. 107, pp. 1-12, (2016).

[21] P. Xu, J. Xing, S. Yao, C. Yang, K. Chen and B. Li, "Energy distribution analysis and multi-objective optimization of a gradual energy-absorbing structure for subway vehicles", *Thin-Walled struct.*, Vol. 115, pp. 255-263, (2017).

[22] L. Ying, M. Dai, S. Zhang, H. Ma and P. Hu, "Multi objective crashworthiness optimization of thin-walled structures with functionally graded strength under oblique impact loading", *Thin-Walled struct.*, Vol. 117, pp. 165-177, (2017).

[23] W. Shen, X. Gu, P. Jiang, J. Hu, X. Lv and L. Qian, "Crushing analysis and multi objective optimization design for rectangular unequal triple-cell tubes subjected to axial loading", *Thin-Walled struct.*, Vol. 117, pp. 190-198 (2017).

[24] X. Zhang, K. Leng and H. Zhang, "Axial crushing of embedded multi-cell tubes", *Int. J. Mech. Sci.*, Vol. 131-132, pp. 459-470, (2017).

[25] X. Zou, G. Gao, H. Dong, S. Xie and G. Chen, T. Tan, "Crashworthiness analysis and structural optimisation of multi-cell square tubes under axial and oblique loads", *Int. J. Crashworthiness*, Vol. 22, No. 2, pp. 129-147, (2017).

[26] A. Eyvazian, T. N. Tran and A. M. Hamouda, "Experimental and theoretical studies on axially crushed corrugated metal tubes", *Int. J. Non-Linear Mech.*, Vol. 101, pp. 86–94, (2018).

[27] S. Chen, H. Yu and J. Fang, "A novel multi-cell tubal structure with circular corners for crashworthiness", *Thin-Walled Struct.*, Vol, 122, pp. 329-343, (2018).

[28] M. Abolfathi and A. Alavi Nia and A. Akhavan attar and M. Abbasi, "Experimental and numerical investigation of the effect of the combined mechanism of circumferential expansion and folding on energy absorption parameters", *Arch. Civ. Mech. Eng.*, Vol. 18, No. 4, pp. 1464-1477, (2018).

[29] M. Abolfathi and A. Alavi Nia, "Optimization of energy absorption properties of thin-walled tubes with combined deformation of folding and circumferential expansion under axial load", *Thin-Walled Struct.*, Vol. 130, pp. 57-70, (2018).

[30] E. Acar, M. Altin and M. A. Güler, "Evaluation of various multi-cell design concepts for crashworthiness design of thin-walled aluminum tubes", *Thin-Walled Struct.*, Vol. 142, pp. 227–235, (2019).

[31] S. Pirmohammad and S. E. Marzdashti, "Multi-objective crashworthiness optimization of square and octagonal bitubal structures including different hole shapes", *Thin-Walled Struct.*, Vol. 139, pp. 126–138, (2019).

[32] X. Zhang and H. Zhang, "Energy absorption of multi-cell stub columns under axial compression", *Thin-Walled Struct.*, Vol. 68, pp. 156-163, (2013).

[33] M. Langseth and O. Lademo, "Tensile and Torsion Testing of AA6060-T4 and T6 Aluminum Alloys at Various Strain Rates", *Technical Report*, (1994).

[34] M. Langseth and O. S. Hopperstad, "Static and dynamic axial crushing of square thin walled aluminum extrusions", *Int. J. Impact Eng.*, Vol. 18, No. 7-8, pp. 949–968, (1996).

[35] Matlab 2016a. http://www.mathworks.com/products/matlab.html, (2020).

How to cite this paper:

F. Kholoosi, S. Jafari and M. Karimi, "Numerical investigation and optimization of the mechanical behavior of thin-walled tubes with combined geometric,", *J. Comput. Appl. Res. Mech. Eng.*, Vol. 11, No. 1, pp. 127-138, (2021).

DOI: 10.22061/JCARME.2020.6737.1860

URL: https://jcarme.sru.ac.ir/?_action=showPDF&article=1418